

Impact of the Dzyaloshinskii-Moriya interaction in strongly correlated itinerant systems

Sergej Schuwalow, Christoph Piefke, and Frank Lechermann

I. Institut für Theoretische Physik, Universität Hamburg, D-20355 Hamburg, Germany

(Received 26 January 2012; revised manuscript received 13 April 2012; published 22 May 2012)

Spin-only approaches to anisotropic effects in strongly interacting materials are often insufficient for systems close to the Mott regime. Within a model context, here the consequences of the low-symmetry relevant Dzyaloshinskii-Moriya (DM) interaction are studied for strongly correlated, but overall itinerant, systems. Namely, we investigate the Hubbard bilayer model supplemented by a DM term at half filling and in the hole-doped regime. As an add-on, further results for the two-impurity Anderson model with DM interaction are also provided. The model Hamiltonians are treated by means of the rotational invariant slave boson technique at the saddle point within a (cellular) cluster approach. Already small values of the anisotropic interaction prove to have a strong influence on the phases and correlation functions with increasing U . An intriguing metallic spin-flop phase is found in the doped bilayer model, and a reduction of the Ruderman-Kittel-Kasuya-Yosida exchange is found in the two-impurity model.

DOI: [10.1103/PhysRevB.85.205132](https://doi.org/10.1103/PhysRevB.85.205132)

PACS number(s): 71.27.+a, 71.23.An, 75.30.Hx, 75.20.Hr

I. INTRODUCTION

The effect of anisotropic magnetic exchange on the atomic level has been recently brought back to a center of interest in condensed-matter physics due to its intriguing importance in, e.g., the search for multiferroic materials,^{1,2} the understanding of complex metallic magnetic surface structures,³ and the phenomenology of topological insulators.⁴ A hallmark step in this research topic has already been performed some fifty years ago by Dzyaloshinskii⁵ and Moriya,⁶ who derived an effective spin-spin interaction term from the spin-orbit coupling in low-symmetry cases, the so-called Dzyaloshinskii-Moriya (DM) interaction. The DM term or more generic magnetic anisotropies are nowadays believed to play furthermore a prominent role in many strongly correlated materials. However nearly exclusively, theoretical studies in this context were in the past bound to pure spin models without itinerancy, leaving the impact of charge fluctuations aside. Yet the latter are surely important, e.g., close to the Mott-critical regime of the metal-insulator transition. Allying the Hubbard model with spin-orbit terms has just recently gained rising interest.^{7,8}

In the present work we aim at a minimal modeling of the influence of the DM interaction in the strongly correlated metallic regime. There are many specific materials problems motivating such a case study, namely, the complex magnetic behavior of doped cuprate systems,^{9–11} manganites,^{12,13} and mono-oxides¹⁴ as well as anisotropic magnetic effects close to the metal-insulator transition in low-dimensional organic compounds¹⁵ or in the context of transition-metal impurities on metallic surfaces.¹⁶ While standard direct and indirect exchange processes favor collinear alignment of the local spins generated in the strongly correlated metallic regime, the DM interaction tends to align the spins in a perpendicular fashion. Thus the competition between the former conventional exchange processes and the DM interaction within an itinerant system shall give rise to nontrivial physics resulting in sophisticated spin arrangements or orderings.

To keep things simple and to build on a somewhat canonical approach, we rely on two basic models, namely, the bilayer model of two coupled single-band Hubbard planes^{17–24} and the two-impurity Anderson model (TIAM).^{25–31} The former

Hamiltonian allows for a DM coupling between two lattice planes in the thermodynamic limit, whereas the latter provides the possibility to study the DM term within a local perspective via interacting impurities coupled to the same bath. Both setups render it possible to investigate nearest-neighbor (NN) correlation functions between sites in an itinerant background. Of course, such modelings are not sufficient to grasp the very details of the above-named materials problems, yet it will be shown that the computed phenomenology is far from trivial and may apply to generic realistic phenomena. One key focus in the context of the Hubbard bilayer lattice is thereby on the competition between the antiferromagnetic (AFM) tendencies driven by direct exchange and the DM term within the metallic state. It will become clear that already rather small values of the DM integral may have a significant influence on the magnetic ordering tendencies in the larger Hubbard U range; i.e., the AFM state is rather sensitive to only minor DM perturbations. A rich phase diagram results from the interplay of kinetic energy, onsite Coulomb interaction, and DM interaction. The latter also has important consequences in the two-impurity model, where its favor for perpendicular spin arrangement severely affects the local-limit competition between singlet-forming Kondo screening and triplet-forming Ruderman-Kittel-Kasuya-Yosida (RKKY) interaction.

In the following we define the model Hamiltonians as well as our mean-field approach in Sec. II. The results for the Hubbard bilayer at half filling and in the hole-doped case are discussed in Sec. III. Some basic observations retrieved from the studies on the two-impurity Anderson model with DM interaction will be presented in Sec. IV.

II. HAMILTONIANS AND THEORETICAL APPROACH

The first problem addressed here consists of two coupled two-dimensional infinite square-lattice planes with one orbital per site, each facing an on-site Coulomb repulsion U (see Fig. 1). In both planes the electron dispersion is defined by identical simple NN hopping t . The interplane coupling is realized via a perpendicular hopping t_{\perp} as well as a DM interaction mediated by the vector integral \mathbf{D} . The model

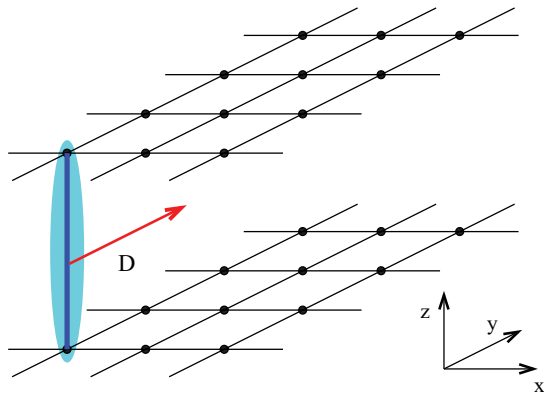


FIG. 1. (Color online) Bilayer model with DM interaction. The vertical blue line represents the interlayer hopping t_{\perp} , which of course is applied at every lattice point, and the ellipse marks the two-site cluster. The DM integral vector \mathbf{D} is chosen to point in the y direction.

Hamiltonian is accordingly written as

$$H_{\text{BL}} = -t \sum_{\substack{\alpha\sigma \\ (i,j)}} (c_{\alpha i\sigma}^{\dagger} c_{\alpha j\sigma} + \text{H.c.}) + t_{\perp} \sum_{i\sigma} (c_{1i\sigma}^{\dagger} c_{2i\sigma} + \text{H.c.}) \\ + U \sum_{\alpha i} n_{\alpha i\uparrow} n_{\alpha i\downarrow} + \sum_i \mathbf{D} \cdot (\mathbf{S}_{1i} \times \mathbf{S}_{2i}), \quad (1)$$

where $c_{\alpha i\sigma}^{(\dagger)}$ creates or annihilates an electron in layer $\alpha = 1, 2$ at lattice site i with spin projection $\sigma = \uparrow, \downarrow$. The $\nu = x, y, z$ component of the spin operator at each site i of an individual layer α is provided by $S_{\alpha i}^{(\nu)} = 1/2 c_{\alpha i\sigma}^{\dagger} \tau_{\sigma\sigma'}^{(\nu)} c_{\alpha i\sigma'}$ with the Pauli matrices $\tau^{(\nu)}$. In general, the vector interaction \mathbf{D} is defined perpendicular to the bond between the involved lattice sites.^{5,6} Since otherwise there is a freedom of choice for the explicit direction, we pick \mathbf{D} to point along the y axis, i.e., $\mathbf{D} = D \mathbf{e}_y$. Note that the DM interaction may only occur if the inversion symmetry is broken. To facilitate this in the present case, one could, e.g., think of an interlayer coupling originally established via oxygen with an angle deviating from 180° .

In the smaller second part of this paper, we take the opportunity to also briefly discuss the well-known two-impurity Anderson model (TIAM) supplemented by a DM interaction between the impurities. We write that model in the form

$$H_{\text{TIAM}} = \sum_{\mathbf{k}\sigma} \varepsilon_{\mathbf{k}} c_{\mathbf{k}\sigma}^{\dagger} c_{\mathbf{k}\sigma} + \varepsilon_d \sum_{i\sigma} n_{i\sigma} \\ + V \sum_{\mathbf{k}i\sigma} (c_{\mathbf{k}\sigma}^{\dagger} d_{i\sigma} + \text{H.c.}) + t_{12} \sum_{\sigma} (d_{1\sigma}^{\dagger} d_{2\sigma} + \text{H.c.}) \\ + U \sum_i n_{i\uparrow} n_{i\downarrow} + \mathbf{D} \cdot (\mathbf{S}_1 \times \mathbf{S}_2), \quad (2)$$

with the impurity-electron operators $d_{i\sigma}^{(\dagger)}$ ($i = 1, 2$), the impurity-level energy ε_d , and the impurity-impurity hopping t_{12} . The bath has associated operators $c_{i\sigma}^{(\dagger)}$ and a dispersion $\varepsilon_{\mathbf{k}}$. The impurity-bath coupling is denoted by V and the Hubbard U is located on the impurities with $n_{i\sigma} = d_{i\sigma}^{\dagger} d_{i\sigma}$. In the present approach the bath is treated explicitly through a three-dimensional simple cubic dispersion with bandwidth $W = 12t$, choosing $t = 0.5$. For the direction of \mathbf{D} again the y axis is selected. The impurities have a common bath, yet V

is assumed here to be k independent and the explicit impurity-impurity distance is formally set to zero. A constant value of $V = -0.5$ is chosen in the present work. Hence only the local part of the RKKY interaction is accessible. Such a modeling is, e.g., important for understanding the local spin interactions between correlated atoms on metallic surfaces,¹⁶ where there is indeed an intriguing interplay between conventional direct exchange, RKKY interaction, Kondo effect, and anisotropic exchange.

For the numerical solution of the model Hamiltonians discussed here, the rotationally invariant slave boson (RISB) formalism^{21,32} in the saddle point approximation is employed, which yields identical results as the generalized infinite-dimension limit of the Gutzwiller variational approach.³³ The RISB methodology amounts to a decomposition of an electron operator $a_{\nu\sigma}$ with generic orbital or site index μ via $a_{\mu\sigma} = \hat{R}[\phi]_{\mu\mu'}^{\sigma\sigma'} f_{\mu'\sigma'}$ into its quasiparticle (QP) part $f_{\mu\sigma}$ and the remaining high-energy excitations carried by the set of slave bosons $\{\phi_{An}\}$. Here A denotes a chosen localized basis state and n relates to the given QP degree of freedom. Two constraints, the first enforcing the normalization of the bosonic content and the second keeping an eye on the match of the bosonic and the fermionic occupation matrix, are established on site average at saddle point through the Lagrange multiplier matrix Λ .²¹ In order to describe interatomic correlations adequately, a two-site (cellular-cluster) framework is used. This cluster connects two NN lattice sites between the layers in the Hubbard bilayer and the two impurities in the TIAM. It amounts to a local cluster approach to the electronic self-energy, whereby $\Sigma_{12}(\omega)$ incorporates terms linear in frequency as well as static renormalizations.²¹ Therewith the low-energy behavior may be adequately expressed and intersite correlation functions as well as multiplet weights on the cluster can be retrieved. Combining the Hubbard model with explicit spin interactions has been already studied within the scope of the Hubbard-Heisenberg model in a spin-isotropic way.³⁴ Due to our cluster approach the direct exchange term driven by t_{\perp}^2/U or t_{12}^2/U is properly included beyond single site in our models. We thus only treat the smaller anisotropic exchange of the DM kind in an explicit way, since it is more difficult to implicitly reproduce it even on the cluster mean-field level from a general spin-orbit term.

Importantly, the formalism allows for full spin and orbital rotational invariance, needed to account for the competition between isotropic and anisotropic interactions. In this respect the slave bosons may become true complex numbers and Λ can be expanded via Pauli matrices in each orbital sector (with allowed off-diagonal terms between these sectors). Albeit the calculations are formally performed at temperature $T = 0$, a small Gaussian smearing for the k point integration introduces a minor T scale. For this reason the energetics are discussed in terms of the free energy F . Note that, in the numerical solution of the TIAM, a three-orbital model is effectively treated within RISB, whereby the bath enters through its band dispersion. Thus the bath degrees of freedom are not integrated out, but are handled explicitly. In principle, a correlated-bath scenario may also be studied; however, we here always keep $U_{\text{bath}} = 0$. Nevertheless, correlation effects are introduced within the bath due to the coupling to the correlated impurities. The investigated half-filled scenario of the model is either achieved

by setting $\varepsilon_d = -U/2$ or through an additional Lagrange multiplier fixing the electron occupation on the bath according to the total filling $N = 3$.

III. HUBBARD BILAYER MODEL

The original Hubbard bilayer without DM interaction has already been addressed in several works,^{17–24} most often concerning the electronic phase diagram when varying the ratio t_\perp/t . Here, however, the main interest lies on the ratio $U/|D|$ for the coupled square-lattice layers with bandwidth $W = 8t$. In the following, we restrict the discussion to cases $t_\perp/t < 1$ with all the energies given in units of the half bandwidth $4t$.

Concerning the electronic phases studied within the current mean-field approach, we restrict the discussion to such long-range orderings that originate from the two-site unit cell. Thus we neglect longer-wavelength orders as realized for, e.g., spin spirals. Such more intricate instabilities are planned to be addressed in more concrete materials-connected future modelings. Here the focus is first on the interplay of the fundamental short-range processes in the strongly correlated metallic regime that drive the eventual long-range order. Note, however, that in the present context the cluster description does not account for intralayer intersite self-energies. In this respect, the antiferromagnetic (AFM) state stabilized at larger Hubbard U is here of the A -type character, i.e., involves two FM layers that are coupled antiferromagnetically.

A. Half-filled case

At half filling, each layer accommodates one electron and the whole system is therefore susceptible to a Mott transition. We study two cases, namely, the one of weakly coupled layers ($t_\perp = 0.025$) and the other with stronger interlayer hopping ($t_\perp = 0.1$).

Figure 2 shows the phase competition within the half-filled model with increasing the Hubbard U . The computations allow for the stabilization of two metallic phases, namely, the paramagnetic (PM) and antiferromagnetic-between-layers (AFM) ones. From the inspection of the free-energy differences it is not surprisingly seen that in general the AFM phase wins over the PM phase at larger U . Thereby a smaller t_\perp , and hence a smaller bonding or antibonding splitting, supports the building up of the AFM phase, in line with dynamical mean-field theory calculations employing quantum Monte Carlo solvers for the impurity problem.^{20,23} A further gain in AFM free energy is observed at fixed U when introducing the DM interaction, but with only marginal shifts of the phase onset toward smaller U . The difference between the two critical $U = U_c$ for the two different t_\perp vanishes with D , while in the case of $D = 0$ the U_c for $t_\perp = 0.1$ is clearly smaller. However, the general evolution of the QP weight $Z = (1 - \partial\Sigma/\partial\omega)^{-1}|_{\omega=0}$ with U does not display strong changes with the introduced anisotropic interaction.

Insight into the local behavior can be gained from the inspection of the respective weights of the various multiplets Γ_p in particle sector p . As, e.g., outlined in detail in Ref. 31, the eigenstates of the local dimer without DM interaction are classified according to the $SU(2)$ symmetry and form triplet

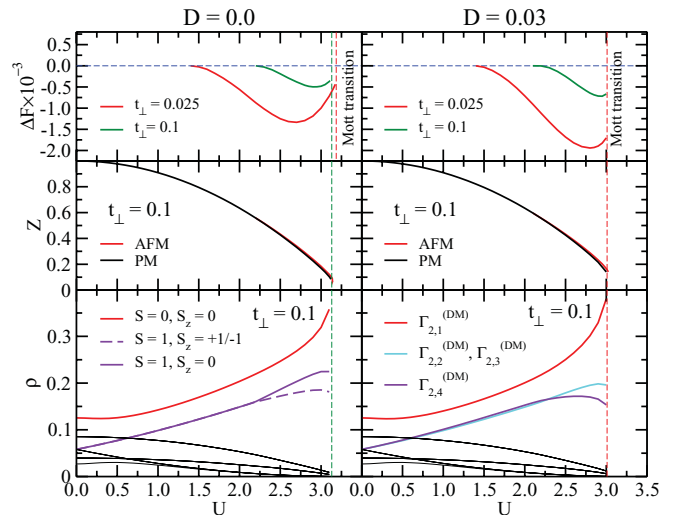


FIG. 2. (Color online) Energetics, QP weight, and multiplet weights with increasing U for the bilayer model at half filling for two values of t_\perp and D , respectively. Free energies are normalized to the one of the PM phase. The thick lines in the multiplet-weights plot correspond to the states in the two-particle sector.

and singlet states in the two-particle sector. The occupation probability ρ_{Γ_p} of these multiplets in the strongly correlated itinerant system is accessible via $\rho_{\Gamma_p} = \sum_{\Gamma'_p} |\phi_{\Gamma_p \Gamma'_p}|^2$. Here $\phi_{\Gamma_p \Gamma'_p}$ denotes the slave boson amplitude connecting Γ_p and Γ'_p in the associated local multiplet basis, obtained from a rotation of the original $\{\phi_{An}\}$. From the induced exchange processes between neighboring sites for $D = 0$, the singlet occupation remains strongest up to the Mott transition, followed by the triplet states (with their degeneracy lifted when entering the AFM phase), as seen in Fig. 2. For $D \neq 0$ the bilayer Hamiltonian Eq. (1) does not commute with $\{S^2, S_z\}$ and thus the former triplet and singlet states are no longer two-particle eigenstates. That is easily understood from the DM interaction favoring a perpendicular alignment of the local spins, in contrast to the originally preferred collinear states. The corresponding new eigenstates $|\Gamma_{p,v}^{(DM)}\rangle$ are still given by a general expansion into Fock states $|n_p\rangle$ through $|\Gamma_{p,v}^{(DM)}\rangle = \sum_n c_{vn}^{(p)} |n_p\rangle$. But now all coefficients $c_{vn}^{(p)}$ are finite for the most probable occupied two-particle state, the modified singlet $|\Gamma_{2,1}^{(DM)}\rangle$. The development of those expansion coefficients with D is documented in Fig. 3. The picture for the multiplet occupations of the modified states shown in Fig. 2 formally looks still very similar.

Figure 4 shows the evolution of the spin moments in the two layers with increasing U . For $D = 0$ only $\langle S_z \rangle$ adopts a nonzero value in the AFM phase, with a steeper increase for larger t_\perp . However, with finite D also a sizable x component of $\langle S \rangle$ shows up and grows until U_c is reached. For the smaller $t_\perp = 0.025$ the value for $\langle S_x \rangle$ even equals the corresponding $\langle S_z \rangle$ magnitude. A lower t_\perp apparently also effectively increases the relative tendency toward the noncollinear spin alignment driven by the DM coupling. Note that the DM interaction not only modifies the AFM phase but has an impact in the PM state as well. There $\langle S_{1,y} S_{2,y} \rangle$ exhibits more AFM-like character and the corresponding

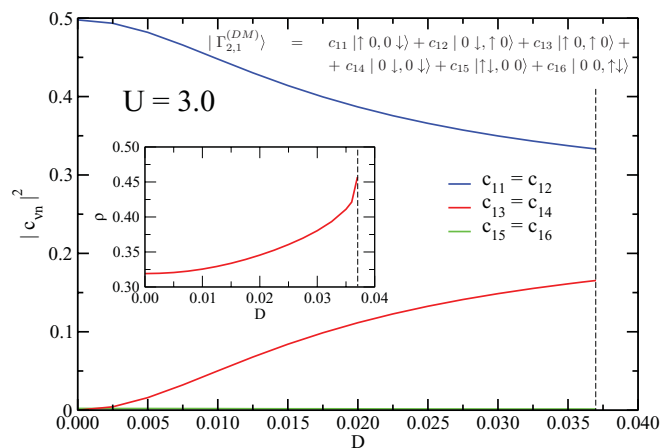


FIG. 3. (Color online) Evolution of the Fock-state contributions for the modified singlet with the highest occupation probability ρ (compare with Fig. 2) for $U = 3$. Note that for $D \neq 0$ this multiplet is no longer an eigenstate of the S^2 and the S_z operator. Inset: D dependence of ρ for that state.

(x, z) correlation functions show minor weakened AFM-like tendencies, both compared to the $D = 0$ case. Close to the Mott transition the larger t_{\perp} results in a stronger (coherent) spin response for $D = 0$, as retrieved from the interlayer spin-correlation functions plotted in Fig. 5. For nonzero D the correlation between the x components, i.e., $\langle S_{1,x} S_{2,x} \rangle$, appears to behave especially more disconnected from the z component for the smaller t_{\perp} .

In order to gain further insight into the impact of the DM term, Fig. 6 depicts explicitly the D dependence for fixed U . The Mott transition itself may be tuned over a rather wide range of the anisotropic interaction. Whereas the spin moment in the x direction shows a strong variation with D , the spin-spin correlations are only weakly dependent thereon. Albeit no resulting $\langle S_y \rangle$ value exists, the correlations along y still

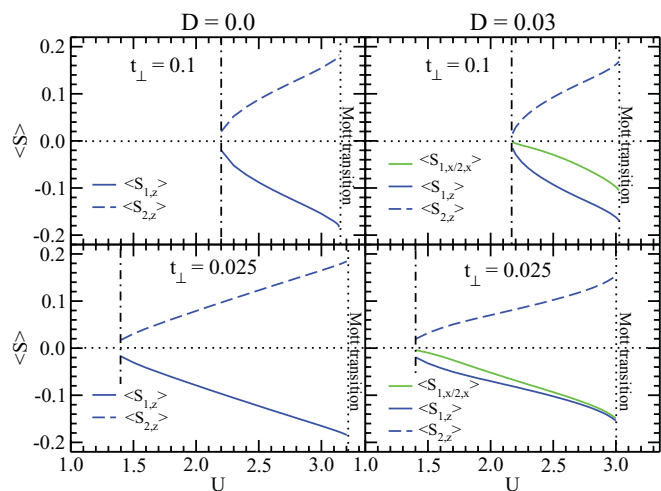


FIG. 4. (Color online) Interaction dependence of the spin expectation values in the AFM phase. Nonzero values of the DM coupling introduce a spin component pointing along the x axis (due to the choice for the direction of the D vector). The vertical dot-dashed lines mark the AFM transition point.

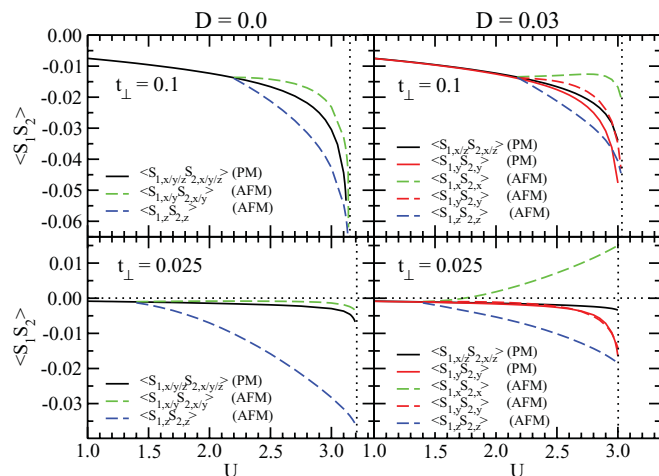


FIG. 5. (Color online) Same as Fig. 4, here for the spin-spin-correlation functions between the layers. Solid lines, PM phase; dashed lines, AFM phase.

appear to gain strongest in magnitude from a larger D . It is also visualized that the angle γ between the local spins on the adjacent layers indeed increasingly deviates from the AFM-ideal 180° with growing DM interaction. Close to the Mott transition, the value $\gamma \sim 100^\circ$ is nearby the DM-ideal value of 90° .

B. Hole-doped case

We now turn to the effects of doping the bilayer model away from half filling. For investigating the simultaneous effects of doping, on-site Coulomb interaction, and intersite DM interaction we set $t_{\perp} = 0.1$ and first fix the Hubbard interaction to $U = 3$. As can be seen from Fig. 2 the value of U puts the system just below the Mott transition at half filling; i.e., strong correlations with the quasiparticle weight $Z \sim 0.2$ exist.

The results of hole doping $\delta = 2 - n$ for the system in the filling range $n \in [1.6, 2.0]$ are summarized in Fig. 7. Let us first

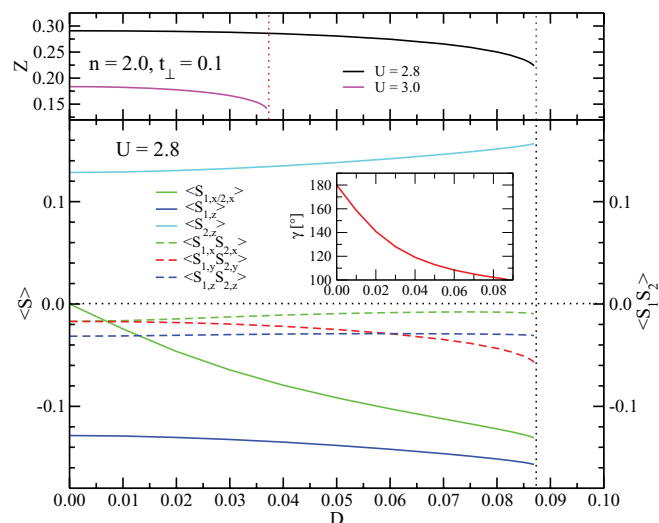


FIG. 6. (Color online) Influence of the DM coupling on the QP weights, spin moments, and spin-spin-correlation functions for the AFM half-filled bilayer model. Inset: evolution of the angle between the spin moments in the two layers.

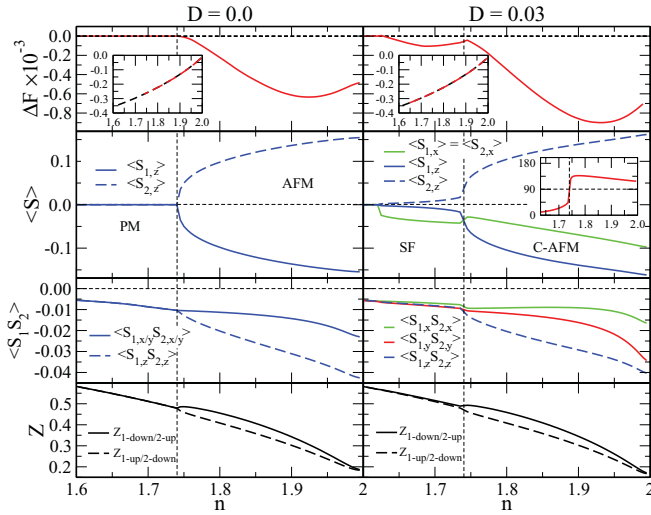


FIG. 7. (Color online) Influence of hole doping on the bilayer model, with and without DM interaction for $t_{\perp} = 0.1$ and $U = 3$. Top insets: free-energy curve, with the region where AFM order is (meta)stable marked in red. C-AFM marks the canted antiferromagnetic phase and SF marks the spin-flop phase. Right-middle inset: evolution of the angle γ between spins.

discuss the $D = 0$ case. Starting from half filling, the system is in the AFM phase for the chosen U value. With increasing δ the order parameter $\langle S_z \rangle$ decreases, until it vanishes close to $n = 1.74$ and the PM phase sets in (at reduced spin-spin correlations and larger QP weight). When including a DM interaction with $D = 0.03$ in the model, the situation becomes more intriguing. Again the AFM phase, now canted in the x direction (and hence designated C-AFM), weakens upon doping from half filling; however, at $n \sim 1.76$ the Hubbard bilayer system shows a first-order phase transition to a metallic spin-flop (SF) phase. The latter one is characterized by the discontinuous jump to a local configuration with an $\langle S_x \rangle$ expectation value *larger* than $\langle S_z \rangle$. This corresponds to an angle γ between the local spins in both layers being lower than 90° , whereas in the C-AFM phase $\gamma \in [90^\circ, 180^\circ]$ holds (see Fig. 8). The strong decrease of γ at the transition point

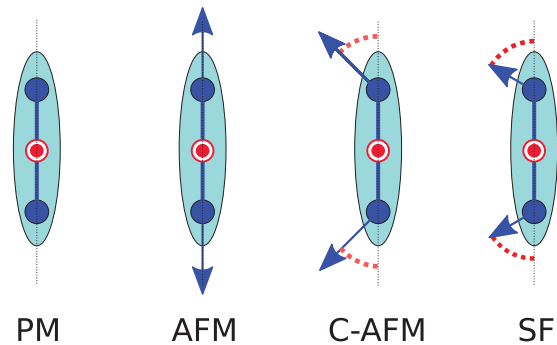


FIG. 8. (Color online) Illustration of the stable local spin configurations according to the local spin-spin angle γ on the interlayer cluster. (a) PM without ordered local moments. (b) AFM with $\gamma = 180^\circ$. (c) C-AFM with γ between 180° (pure AFM ordering) and 90° (pure DM ordering). (d) SF with $\gamma < 90^\circ$, i.e., weak ferromagnetism with strong canting.

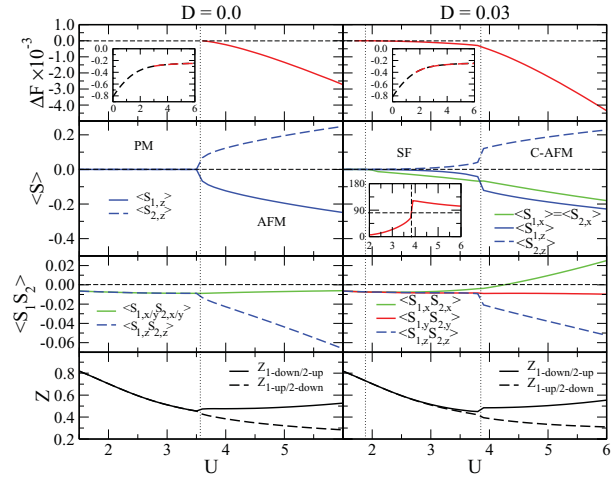


FIG. 9. (Color online) Phase diagram with U for the doped Hubbard bilayer at filling $n = 1.7$ (compare with Fig. 7). Insets: free-energy curves and the interaction-dependent spin-spin angle γ .

may be observed in the inset of Fig. 7. Hence the SF phase displays weak ferromagnetism due to strong canting. Note that neither the spin-correlation functions nor the diagonal Z values show a strong signature therein. The SF phase transforms into the usual PM phase at $n \sim 1.62$.

In addition to the doping scan, Fig. 9 displays the various phases emerging with increasing Hubbard interaction U for fixed hole doping $\delta = 0.3$, i.e., $n = 1.7$. Without the DM interaction, the standard picture of a stable PM phase at small U and a stable AFM phase at larger U ($U > 3.58$) remains vital. Note that the U values for AFM stabilization are well above the Mott critical U at half filling. Introducing D stabilizes the metallic SF phase for $1.9 < U < 3.85$, accompanied with the jump in the angle γ toward lower values. Therewith the onset of AFM order takes place at slightly larger U than for $D = 0$. Hence the finite D enables specific magnetic ordering in a Coulomb interacting regime that is originally not susceptible to such order. Only the z component of the spin-correlation function shows a discontinuous behavior at the SF/C-AFM phase boundary.

IV. TWO-IMPURITY ANDERSON MODEL

The TIAM²⁵⁻³¹ belongs to the set of canonical models in the physics of strong electronic correlations, believed to be relevant for the understanding of heavy-fermion systems.³⁵ Via the coupling of the impurities to a bath it contains the single-impurity Kondo physics and as a competitor also the RKKY mechanism acting between the impurities. The latter originates from the effective exchange introduced through the impurity coupling to the same bath. In some works^{18,31} this type of exchange interaction between sites is discussed in the context of two impurities coupled to different baths (similar to the bilayer architecture). But here we try to separate the exchange in an indirect (“RKKY”) one, stemming from effective exchange via the bath, and a direct term, resulting, e.g., from an explicit hopping amplitude t_{12} between the impurities [see Eq. (2)].

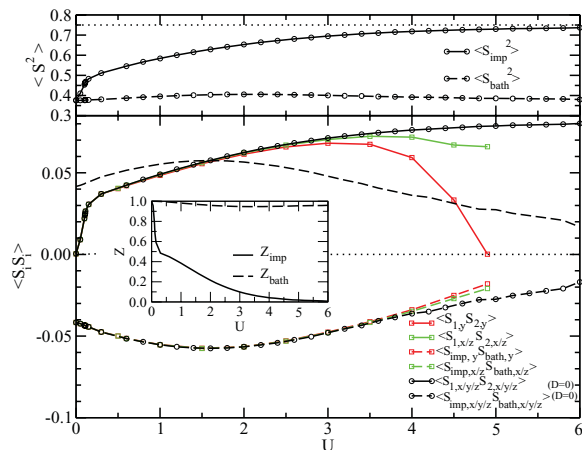


FIG. 10. (Color online) Interaction-dependent spin-correlation functions for the TIAM with $t_{12} = 0$. Top: $\langle S^2 \rangle$ for $D = 0$. Bottom: spin-spin correlations for $D = 0$ (circles) and $D = 0.05$ (squares). The dashed dark line without circles is the $\langle S_{\text{imp}} S_{\text{bath}} \rangle$ correlation function mirrored at the zero line.

Figure 10 shows the RISB results for the spin-correlation functions of the fundamental model with $t_{12} = D = 0$. Thus the two impurities are only coupled via the bath and exchange can only be mediated therewith. The expectation value $\langle S^2 \rangle = S(S + 1)$ on the impurity quickly rises with U due to the formation of the local moment. It approaches the value $3/4$, corresponding to the full $S = 1/2$ limit, at large interaction strength. With increasing U a local Fermi liquid is established with a small quasiparticle weight Z_{imp} (see inset, Fig. 10). The competition between the Kondo screening and the RKKY interaction may be observed from inspection of the spin-spin correlations. From Fig. 10 it is obvious that $\langle S_{\text{imp}} S_{\text{bath}} \rangle$, i.e., the correlation between a single impurity and the bath, is always of AFM character with a maximum close to $U_K \sim 1.6$. On the other hand the interimpurity correlation $\langle S_1 S_2 \rangle$ is exclusively of the FM kind and shows monotonic increase with U . The former is associated with the singlet-forming tendencies due to Kondo screening, whereas the latter signals triplet-forming tendencies because of the FM RKKY exchange within the local limit. Close to U_K the absolute value of the local RKKY correlation exceeds the singlet-forming amplitude between impurity and bath. The system at larger U is then dominated by the RKKY interaction.^{26,30,31} Within a conventional Schrieffer-Wolff mapping³⁶ for the Kondo coupling via $J_K = 8V^2/U$, a similar crossover regime would follow also from simple estimates through the associated exchange interactions, for if we understand the RKKY interaction as a second-order process, i.e., $J_{\text{RKKY}} \sim J_K^2$, then here the two exchange integrals become equivalent for $U = 2$, which is the order of magnitude from the numerics. With increasing impurity-bath coupling V the crossover shifts to larger U , since J_K^2 profits more strongly therefrom. However, note that with our bath bandwidth $W = 6$ the present TIAM is surely not in the Kondo-Hamiltonian limit ($U \gg W$) for the studied interaction range.²⁸ Turning on a finite DM term of size $D = 0.05$ has nearly no effect at small U . However, for larger Hubbard interaction rather strong modifications occur, especially for the interdimer function $\langle S_{1,y} S_{2,y} \rangle$. Remember that the D vector also points in the y

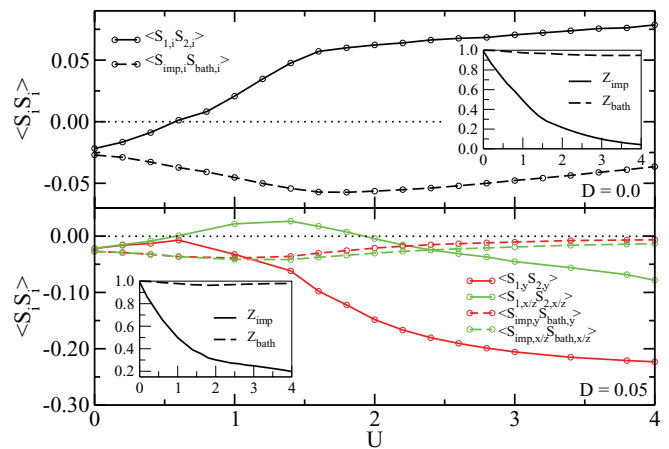


FIG. 11. (Color online) Interaction-dependent spin-spin correlations for the TIAM with $t_{12} = 0.2$, with and without DM interaction.

direction. Thus an intricate spin-spin coupling scenario arises at large U , with still FM alignment in the (x, z) axes and near AFM alignment in the y axis. For $U > 5$ our mean-field approach yields net local moments in the presence of a finite D ; i.e., a paramagnetic solution is no longer stabilizable. It would thus be very interesting to study the large- U regime of this model beyond mean field (e.g., with the numerical renormalization-group approach utilized in Ref. 30).

In addition to the basic model with vanishing interimpurity hopping, Fig. 11 exhibits the resulting spin-correlation functions for the TIAM with $t_{12} = 0.2$. Now both $\langle S_{\text{imp}} S_{\text{bath}} \rangle$ and $\langle S_1 S_2 \rangle$ display AFM correlations in the weakly interacting limit. This is understood from the direct exchange integral $J_{\text{dir}} = 4t_{12}^2/U$ originating from the introduced dimer coupling. With increasing U the correlation functions develop rather similarly as for $t_{12} = 0$, yet the overall magnitude is somewhat reduced at small interaction strength. Hence there the direct exchange weakens both impurity Kondo screening (due to the stronger interimpurity link) as well as FM RKKY interaction (since the direct exchange favors AFM behavior). But the crossover point of domination for these processes does not seem to change much with the introduced t_{12} . Of course, a very large t_{12} should rank the direct exchange above the other mechanisms; however, here we do not investigate this model limit. Finally, when introducing the DM term to the model, effectively four different exchange mechanisms compete with each other: impurity Kondo, RKKY, direct, and DM. The latter has indeed again significant effect on the spin correlation between the impurities. For already moderate values of U the dominance of the FM RKKY is lost, turning the system into AFM-like interimpurity correlations for $U > 2$. Thus also here the DM interaction severely influences the magnetic correlations for isolated impurities within an itinerant background. It appears to strengthen the singlet-forming tendencies (with stronger response in the D direction) in an otherwise triplet-favoring RKKY system at short-range distance.

V. SUMMARY

A theoretical investigation of effects stemming from the Dzyaloshinskii-Moriya interaction in itinerant systems with strong electronic correlations was presented in this work. In

order to study the principle physics on the lattice as well as in the local limit, we elaborated on two prominent model systems, namely, the Hubbard bilayer and the one defined by the two-impurity Anderson Hamiltonian. In both cases substantial influence of the DM interaction is found, especially at large coupling, where the strong renormalization enhances the impact. The half-filled Hubbard bilayer displays large out-of-axis spin components close to the Mott transition that may severely influence the magnetic response in an applied field. Intriguing phenomena in this respect are, e.g., observed in quasi-two-dimensional organic compounds.¹⁵ At finite hole doping and larger U , the bilayer system with DM interaction exhibits the emergence of a metallic spin-flop phase between the AFM phase at half filling and the PM phase at stronger doping. This finding is of vital importance for many doped Mott systems with anisotropies. For instance, it is well known that the hole-doped layered cuprates display puzzling phases between the AFM region and the superconducting dome and that the DM interaction is not completely negligible at low energy.^{9–11} Notably it would be very interesting to investigate in some detail whether there is a closer connection between our model results and the observation of spin-glass behavior in these systems.³⁷

The TIAM is very relevant not only in the context of heavy fermions but, e.g., also for isolated atoms on metallic

surfaces. In either case, anisotropic spin terms such as the DM interaction exist in many realistic representants in nature. It results from our studies that the DM term becomes an important player in the hierarchy of relevant exchange processes in these contexts. In the local limit it works against the FM tendencies of the RKKY interaction and promotes the singlet formation between the impurities at large local Coulomb interactions. Further research along these lines, e.g., by going beyond mean field, including the complete k dependence of the impurity-bath coupling or tailoring the modeling toward concrete materials systems, is of vital interest to account for generic exchange processes in the strongly correlated itinerant regime.

ACKNOWLEDGMENTS

We thank M. Potthoff and D. Grieger for helpful discussions. Financial support from the Free and Hanseatic City of Hamburg in the context of the Landesexzellenzinitiative Hamburg as well as from the DFG project SPP 1386 is gratefully acknowledged. Computations were performed at the local computing center of the University of Hamburg as well as the North-German Supercomputing Alliance (HLRN) under Grant No. hhp00026.

- ¹C. Ederer and N. A. Spaldin, *Phys. Rev. B* **71**, 060401(R) (2005).
²D. Khomskii, *Physics* **2**, 20 (2009).
³M. Bode, M. Heide, K. von Bergmann, P. Ferriani, S. Heinze, G. Bihlmayer, A. Kubetzka, O. Pietzsch, S. Blügel, and R. Wiesendanger, *Nature (London)* **447**, 190 (2007).
⁴J.-J. Zhu, D.-X. Yao, S.-C. Zhang, and K. Chang, *Phys. Rev. Lett.* **106**, 097201 (2011).
⁵I. Dzyaloshinskii, *J. Phys. Chem. Solids* **4**, 241 (1958).
⁶T. Moriya, *Phys. Rev.* **120**, 91 (1960).
⁷D. Pesin and L. Balents, *Nature Phys.* **6**, 376 (2010).
⁸Z. Y. Meng, T. C. Lang, S. Wessel, F. F. Assaad, and A. Muramatsu, *Nature (London)* **464**, 847 (2010).
⁹T. Thio, T. R. Thurston, N. W. Preyer, P. J. Picone, M. A. Kastner, H. P. Jenssen, D. R. Gabbe, C. Y. Chen, R. J. Birgeneau, and A. Aharony, *Phys. Rev. B* **38**, 905(R) (1988).
¹⁰D. Coffey, T. M. Rice, and F. C. Zhang, *Phys. Rev. B* **44**, 10112 (1991).
¹¹V. Juricic, M. B. S. Neto, and C. M. Smith, *Phys. Rev. Lett.* **96**, 077004 (2006).
¹²K. Hirota, Y. Moritomo, H. Fujioka, M. Kubota, H. Yoshizawa, and Y. Endoh, *J. Phys. Soc. Jpn.* **67**, 3380 (1998).
¹³J. F. Mitchell, D. N. Argyriou, A. Berger, K. E. Gray, R. Osborn, and U. Welp, *J. Phys. Chem. B* **105**, 10731 (2001).
¹⁴I. V. Solovyev, A. I. Liechtenstein, and K. Terakura, *Phys. Rev. Lett.* **80**, 5758 (1998).
¹⁵F. Kagawa, Y. Kurosaki, K. Miyagawa, and K. Kanoda, *Phys. Rev. B* **78**, 184402 (2008).
¹⁶L. Zhou, J. Wiebe, S. Lounis, E. Vedmedenko, F. Meier, S. Blügel, P. H. Dederichs, and R. Wiesendanger, *Nature Physics* **6**, 187 (2010).
¹⁷W. Ziegler, P. Dieterich, A. Muramatsu, and W. Hanke, *Phys. Rev. B* **53**, 1231 (1996).
¹⁸G. Moeller, V. Dobrosavljević, and A. E. Ruckenstein, *Phys. Rev. B* **59**, 6846 (1999).
¹⁹A. Fuhrmann, D. Heilmann, and H. Monien, *Phys. Rev. B* **73**, 245118 (2006).
²⁰S. S. Kancharla and S. Okamoto, *Phys. Rev. B* **75**, 193103 (2007).
²¹F. Lechnermann, A. Georges, G. Kotliar, and O. Parcollet, *Phys. Rev. B* **76**, 155102 (2007).
²²K. Bouadim, G. G. Batrouni, F. Hébert, and R. T. Scalettar, *Phys. Rev. B* **77**, 144527 (2008).
²³H. Hafermann, M. I. Katsnelson, and A. I. Lichtenstein, *Europhys. Lett.* **85**, 37006 (2009).
²⁴T. Yoshikawa and M. Ogata, *Phys. Rev. B* **79**, 144429 (2009).
²⁵C. Jayaprakash, H. R. Krishna-Murthy, and J. Wilkins, *J. Appl. Phys.* **53**, 2142 (1982).
²⁶R. M. Fye, J. E. Hirsch, and D. J. Scalapino, *Phys. Rev. B* **35**, 4901 (1987).
²⁷B. A. Jones, B. G. Kotliar, and A. J. Millis, *Phys. Rev. B* **39**, R3415 (1989).
²⁸R. M. Fye and J. E. Hirsch, *Phys. Rev. B* **40**, 4780 (1989).
²⁹A. Schiller and V. Zevin, *Ann. Phys.* **508**, 363 (1996).
³⁰S. Nishimoto, T. Pruschke, and R. M. Noack, *J. Phys.: Condens. Matter* **18**, 981 (2006).
³¹M. Ferrero, P. S. Cornaglia, L. DeLeo, O. Parcollet, G. Kotliar, and A. Georges, *Phys. Rev. B* **80**, 064501 (2009).
³²T. Li, P. Wölfle, and P. J. Hirschfeld, *Phys. Rev. B* **40**, 6817 (1989).
³³J. Bünemann, W. Weber, and F. Gebhard, *Phys. Rev. B* **57**, 6896 (1998).
³⁴B. J. Powell and R. H. McKenzie, *Phys. Rev. Lett.* **94**, 047004 (2005).
³⁵S. Doniach, *Physica B* **91**, 231 (1977).
³⁶J. R. Schrieffer and P. A. Wolff, *Phys. Rev.* **149**, 491 (1966).
³⁷C. Niedermayer, C. Bernhard, T. Blasius, A. Golnik, A. Moodenbaugh, and J. I. Budnick, *Phys. Rev. Lett.* **80**, 3843 (1998).